UNITED STATES ATOMIC ENERGY COMMISSION

UCRL-2380

THE SCATTERING OF ELECTRONS BY ATOMIC NUCLEI (thesis)

By
Peter C. Giles

September 1953

Radiation Laboratory
University of California, Berkeley

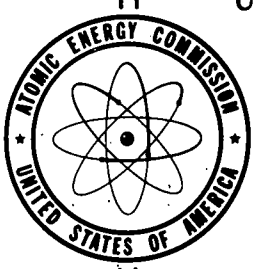

Technical Information Service, Oak Ridge, Tennessee

DISCLAIMER

Subject Category, PHYSICS.
Work performed under Contract No. W-7405-eng-48.

Printed in USA, Price 35 cents. Available from the Office of Technical Services, Department of Commerce, Washington 25, D. C.

AEC, Oak Ridge, Tenn.-W40452

THE SCATTERING OF ELECTRONS BY ATOMIC NUCLEI

Peter C. Giles
(Thesis)

Radiation Laboratory, Department of Physics
University of California, Berkeley, California

September, 1953

ABSTRACT

The scattering of electrons and positrons at both large and small angles has been studied by observing their tracks as they penetrate nuclear emulsions. The measurements of the large-angle scattering ($> 4^{\circ}$) of both ~40-Mev electrons and positrons have been compared with the Rutherford scattering law. Within the statistics available, fair agreement was found with the relativistic Rutherford formula.

A scheme of analysis for gamma-ray spectra based upon multiple scattering measurements of the pair-production electrons has been developed. It is applied to the determination of the energy spectrum of gamma-rays emitted by a beryllium target under bombardment by 330-Mev protons.

THE SCATTERING OF ELECTRONS BY ATOMIC NUCLEI

Peter C. Giles
(Thesis)

Radiation Laboratory, Department of Physics
University of California, Berkeley, California

September, 1953

I. INTRODUCTION

The study of the interaction of charged particles with matter has been an historically productive means of investigating either phenomena associated with the penetrated matter or properties of the particle itself. Investigations of the first kind have demonstrated the existence of a massive atomic nucleus of positive charge, and more recently -- with the aid of high energy accelerators -- have provided valuable information concerning the structure of the nucleus. Investigations of the second kind made possible the discovery of the positron and of mesons, and produced quantitative measurements of the mass, charge, and spin of many particles.

The theoretical description by quantum electrodynamics of electrons and positrons and their behavior is fairly complete. While up to a few Mev there is considerable experimental verification of the theory, there are insufficient corroborating data at the higher energies. Recent cosmic-ray work, however, has indicated that the theory may be valid well into the high-energy region. It is obviously important to investigate further the behavior of high-energy electrons and positrons as they penetrate matter.

In this paper investigations of two aspects of the scattering of electrons by nuclei are described. In a study of the first kind mentioned above, a comparison is made of the scattering at large angles of ~40-Mev electrons with that of ~40-Mev positrons. In a study of the second kind, empirical information about the small-angle, or multiple, scattering of electrons is applied to determining the energy spectrum of photons emitted by a beryllium target under bombardment by 330-Mev protons. This is done by measuring the multiple scattering of the electrons and positrons, which are created in pairs by these photons, as they penetrate the nuclear emulsion.

Incidentally to the study of the large-angle scattering a number of positron disappearances were observed. An analysis of these was performed and a cross section is quoted and compared with the theoretical predictions of positron annihilation in flight.

II. LARGE-ANGLE SCATTERING

A. Scattering Theory

A theoretical expression for the scattering of electrons by nuclei was first derived by Lord Rutherford. For consideration of their traversal of a finite thickness of matter, the scattering is treated as having two components. The first is small-angle or multiple scattering, which is properly described by a statistical analysis, and the second is large-angle, single nuclear scattering. The expression for the scattering is found to involve a Gaussian term for the small-angle scattering, plus a large-angle tail closely approximated by the Rutherford formula.

The quantum-mechanical analysis of scattering was first presented by Mott in 1929.[1] He was able to transform Dirac's expression describing the electron into one in the form of Schroedinger's equation, with the potential term amended by spin and relativistic terms. Use of the simple Schroedinger equation in describing scattering yields the charge-independent Rutherford scattering law, i.e., the $\csc^4 \frac{\theta}{2}$ relation. However, the introduction into the potential term of relativistic and spin terms leaves the resulting expression no longer charge-independent,[2] predicting an excess of electron over positron scattering at large angles. As summarized by Lipkin,[3] the expression for the ratio of electron to positron scattering is:

$$R = 1 + \frac{2\pi\alpha\beta \sin\frac{\theta}{2}\left(1 - \sin\frac{\theta}{2}\right)}{1 - \beta^2 \sin^2\frac{\theta}{2} - \pi\alpha\beta \sin\frac{\theta}{2}\left(1 - \sin\frac{\theta}{2}\right)} \qquad \text{where} \quad \alpha = \frac{Ze^2}{\hbar c}, \quad \beta = \frac{v}{c} \qquad (1)$$

According to Lipkin, a simple picture of this effect is obtained by regarding the positron and electron as having magnetic moments plus point charges. Owing to the existence of a second-order effect involving the dipole component parallel to the direction of flight, on the statistical average the particle will be attracted to the nucleus. Hence the resultant repulsive force on the positron is lessened, and the resultant attractive force on the electron is increased, giving rise to slightly larger scatters for the electrons than for positrons of the same impact parameter.

B. Experimental Procedure

Electrons and positrons were obtained as pairs created by the 300-Mev synchrotron bremsstrahlung beam as it penetrated a tantalum target. Their nominal energies were 38.5 Mev and 36.1 Mev, respectively, as determined from multiple-scattering measurements. The particles were magnetically separated by a pair spectrometer whose field was effectively constant over their entire path. The magnetic field was calibrated with a proton moment fluxmeter. The spectrometer magnet was optically aligned with the beam by a telescope. The magnetic field direction was determined from the direction of force on a current-carrying wire. Detectors were 200-micron nuclear emulsion plates (G-5) ; incident particles of desired energies were obtained by the appropriate choice of positions for these plates. The plates were positioned during the exposure in such a way that the particles entered at $\sim 5^{\circ}$ to the surface of the emulsion and perpendicularly to the leading edge of the plate. (see Fig. 1).

Electron-sensitive G-5 type emulsions accumulate with time many background slow-electron tracks. Therefore it was necessary to eradicate their latent images immediately before exposure. After the exposure the plates were developed by a temperature cycle process. The eradication, exposure, and development of the plates are described in detail by Violet.[4]

The plates were scanned under 530-power magnification with a Bausch and Lomb microscope equipped with a special stage designed to read translations to ~1 micron. Only tracks entering within $\sim 3^{\circ}$ of the normal to the leading edge were selected for scanning. Track lengths were measured with the special microscope stage. Tracks were not scanned and events were not

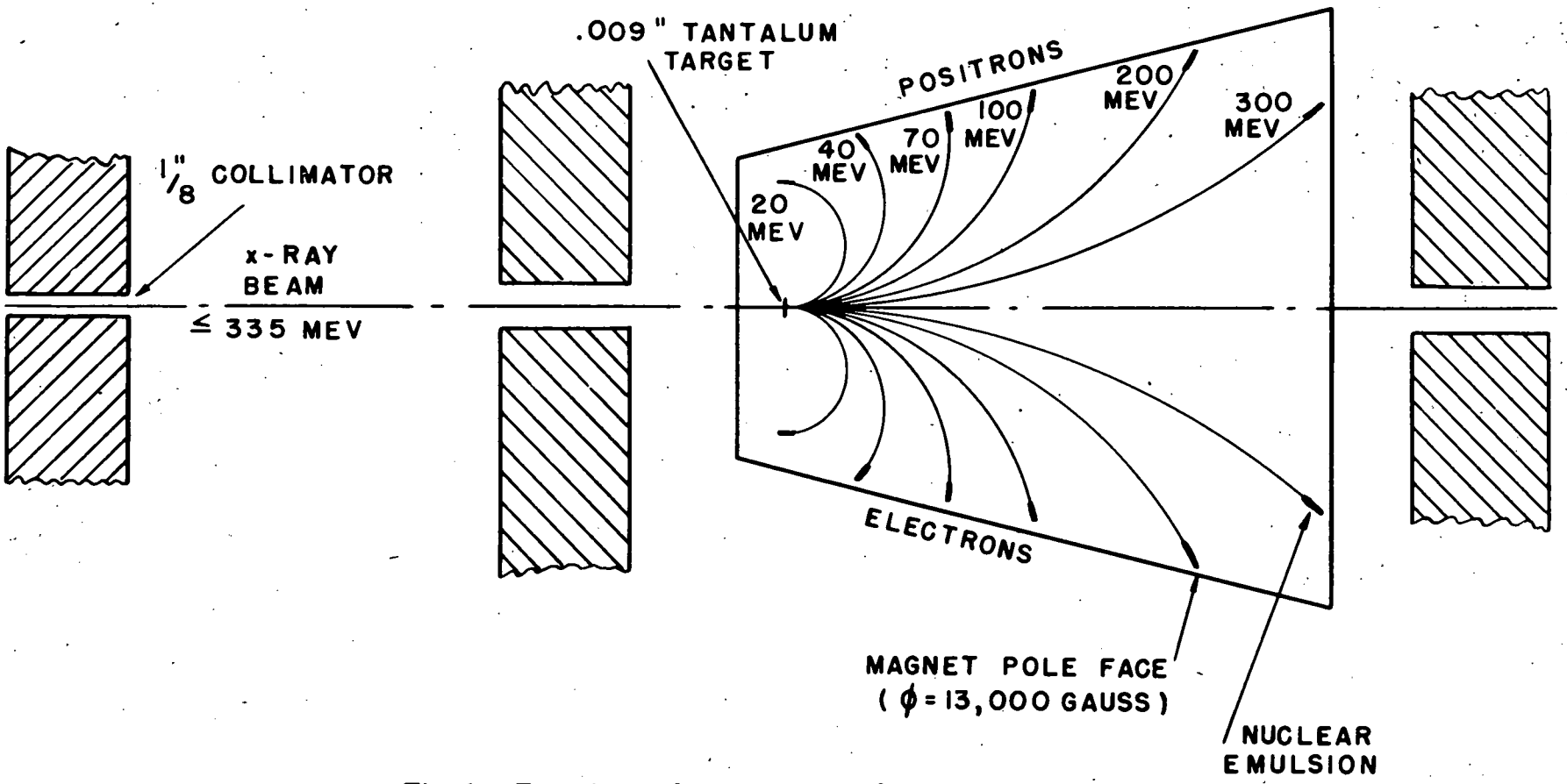

Fig. 1—Experimental arrangement of pair spectrometer.

recorded within 10 microns of the air-emulsion surface. In the acceptable region scatters were recorded in terms of their horizontally projected angles. The recording of angles in terms of their horizontal projection eliminates any uncertainty in the shrinkage factor of the emulsion. This shrinkage occurs during the drying after processing, because a large volume of silver halide is removed from the emulsion by the fixer.

Measurements of scatters were made in terms of the sine of the angle with a 100-division reticle placed in one eyepiece. By repeated measurements of several scatters the standard deviation, σ_s, of the sine, due to observer resolution, was ascertained to be 6.8×10^{-3}. Three plates were scanned: one that had been exposed to positrons, and two to electrons. The electron plates and a portion of the positron plate were scanned until equal numbers of scatters greater than 4° were obtained. In addition, another portion of the positron plate was scanned and scatters recorded greater than 6°. The choice of the minimum angle was a compromise which afforded the most rapid gathering of statistics without allowing resolution effects to distort the results. Scanning of both portions of the positron plates was facilitated by measuring the length of only every tenth track. From the distributions of track lengths, the probable error in track length in the portion scanned for events greater than 4° was found to be 2.0 percent, and that for the portion scanned for events greater than 6° was 2.3 percent. The total track length and the distribution of angles were then compiled for the electrons and positrons. The largest scatter observed was one of $68\text{-}1/2^\circ$ by an electron. It is shown in Fig. 2. The observed distributions of scatters for both particles are shown in Fig. 3.

C. Data Analysis

1. Transformation from Solid Angle to Horizontally Projected Angle

In order to compare properly the observed data with theoretical expectations, the theoretical expression for the angular distribution must be expressed in terms of the horizontally projected angle. The analysis follows Barkas.[5] A good approximation for the theoretical scattering is given by the relativistically corrected Rutherford expression

$$\sigma(\theta)\, d\Omega = A \csc^4 \frac{\theta}{2}\, d\Omega \qquad (2)$$

$$\text{where } A = \left(\frac{Z e^2}{2 m_o c^2}\right)^2 \left(\frac{1 - \beta^2}{\beta^4}\right)$$

$\sigma(\theta)$ is the cross section for scattering at an angle θ. See Fig. 4.

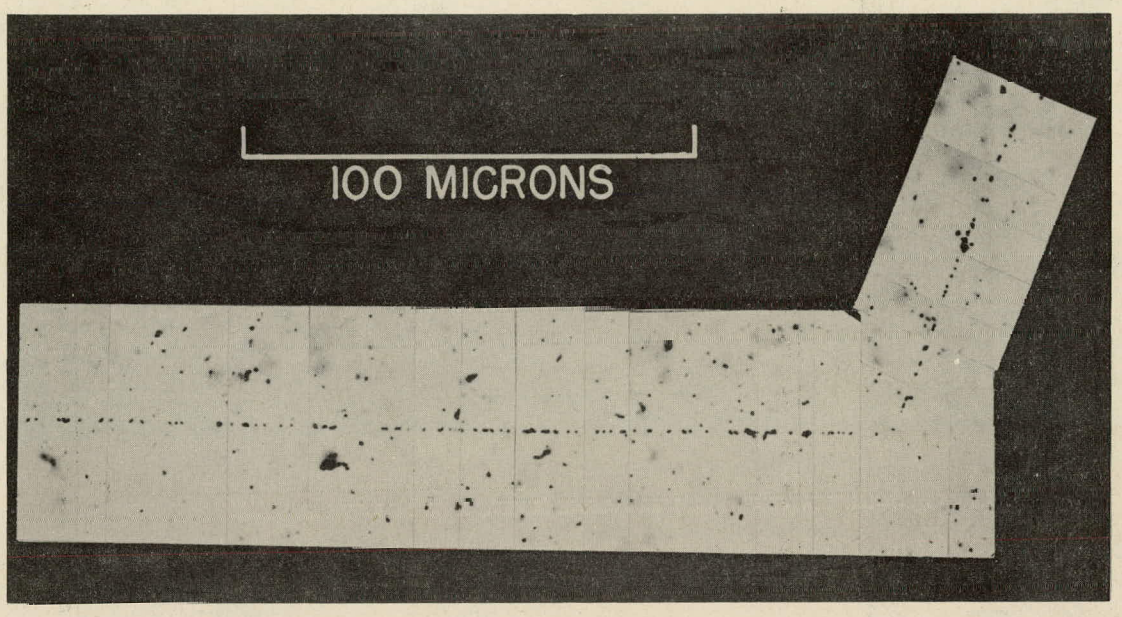

Fig. 2 — Photomicrograph mosaic of an electron-nuclear scatter. A 40-Mev electron enters at left and is scattered to upper right at an angle of 68.5°.

10

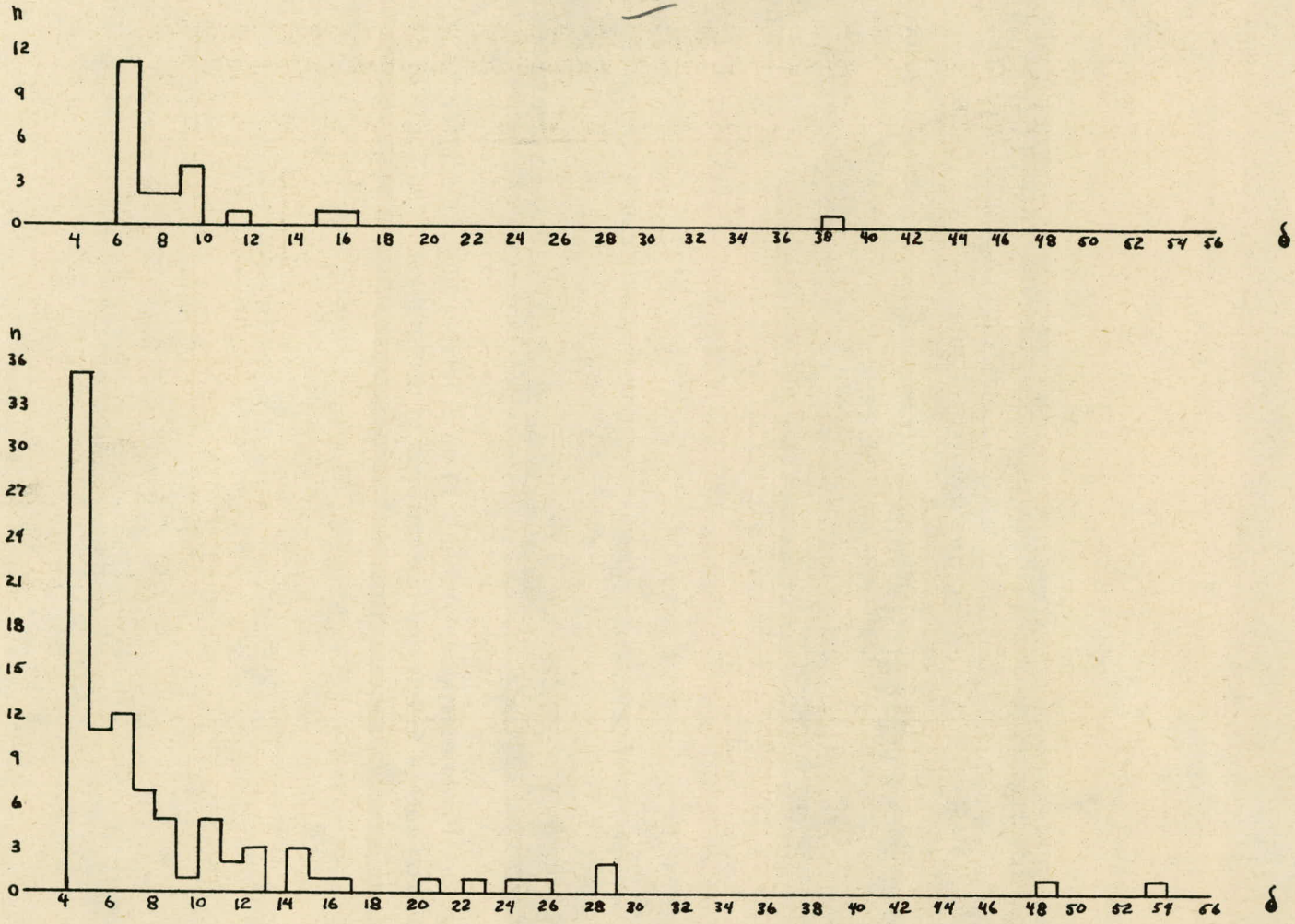

Fig. 3A—Histogram of the number of positron-nuclear scatters vs the angle in degrees. The upper portion shows those found in the area scanned for scatters > 6 degrees.

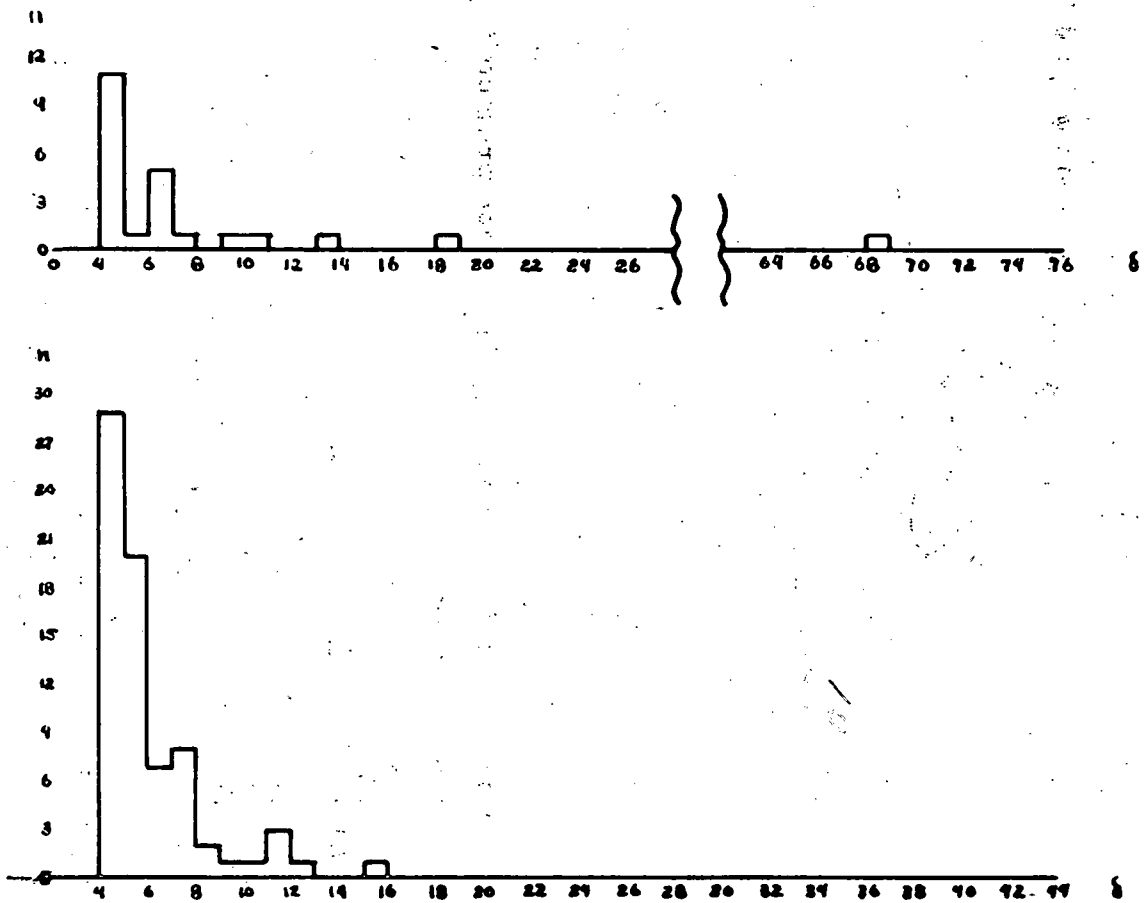

Fig. 3B—Histogram of the number of electron-nuclear scatters vs the angle in degrees. The results of both plates "A" and "B" are shown.

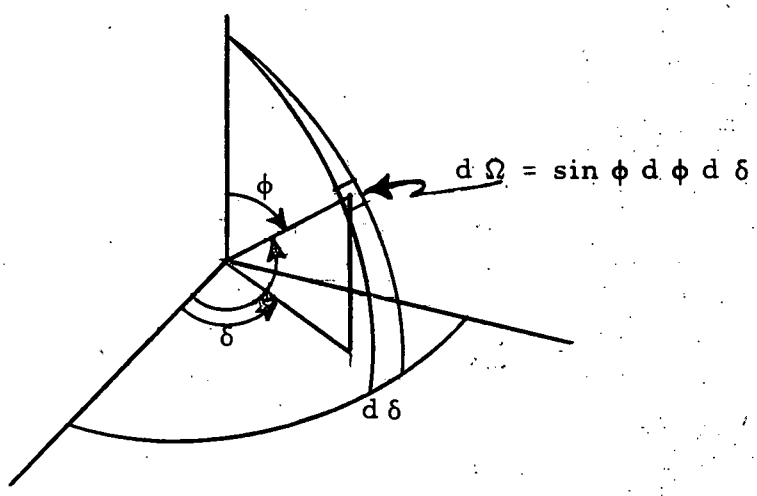

Fig. 4

In order to transform this expression into terms of the plane projected angle δ, the Rutherford expression is written as:

$$\sigma(\theta)\, d\Omega = \frac{4A}{(1 - \cos\theta)^2}\, d\Omega \quad .$$

Using the relation $\cos\theta = \cos\delta \sin\phi$, we see that

$$\sigma(\theta)\, d\Omega = \frac{4A \sin\phi\, d\phi\, d\delta}{(1 - \cos\delta \sin\phi)^2} \quad .$$

Integration over ϕ gives the total probability of scattering into the plane projected angle δ :

$$W(\delta)\, d\delta = 4A\, d\delta \int_0^{\pi} \frac{\sin\phi\, d\phi}{(1 - \cos\delta \sin\phi)^2} \quad .$$

Letting $u = 1 - \cos \quad \sin \phi$,

$$W(|\delta|)\, d\delta = \frac{8 A\, d\delta}{\cos \delta} \int_1^{1 - \cos \delta} \frac{(1 - u)\, du}{u^2 \sqrt{\cos^2 \delta - (1 - u)^2}}$$

$$= \frac{16 A\, d\delta}{\cos \delta} \left[1 + (\pi - |\delta|) \cot |\delta|\right] . \qquad (3)$$

For the purposes of this experiment the integrated cross section above δ_o will be considered:

$$\int_{|\delta_o|}^{\pi} W(|\delta|)\, d\delta = 8A \left[\cot |\delta_o| + (\pi - |\delta_o|) \csc^2 \delta_o\right] . \qquad (4)$$

It can now be shown that the integrated cross section taken with respect to the space angle θ is twice the integrated cross section taken with respect to the horizontally projected angle δ, provided the lower limits of integration, δ_o and θ_o, are small and equal. The integrated cross section with respect to the space angle θ is given by

$$\int_{\theta_o}^{\pi} A \csc^4 \frac{\theta}{2}\, d\Omega = 2\pi A \int_{\theta_o}^{\pi} \frac{\sin\theta\, d\theta}{\sin^4 \frac{\theta}{2}} = 4\pi A \left[\frac{1}{\sin^2 \frac{\theta_o}{2}} - 1\right]$$

using $d\Omega = 2\pi \sin\theta\, d\theta$.

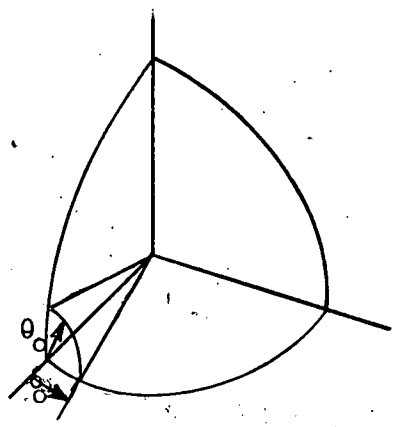

Fig. 5

The ratio of the two expressions for the cross section is:

$$R = \frac{4\pi A \left[\frac{1}{\sin^2 \theta_o/2} - 1\right]}{8 A \left[\cot|\delta_o| + (\pi - |\delta_o|) \csc^2 \delta_o\right]}$$

For $\theta_o = \delta_o$ the limit of R as δ_o approaches zero is seen to be 2.

2. Calculation of A.

Since the scattering cross section is additive in a mixture of elements, such as nuclear emulsions, the total cross section in emulsion is the sum of the individual cross sections for each element. The constant A then, becomes

$$A = \sum_i N_i Z_i^2 \left(\frac{e^2}{m_o c^2}\right)^2 \frac{1}{4} \frac{1 - \beta^2}{\beta^4} .$$

The summation of $N_i Z_i^2$ is found, from information supplied by the manufacturer, to be 37.0×10^{24} cm^{-3}.

If the particle energies are assumed to be normally distributed about the mean energy E with standard deviation σ, the effective A becomes

$$A = \sum_i N_i Z_i^2 \left(\frac{e^2}{m_o c^2}\right)^2 \frac{1}{4} \int \frac{1 - \beta^2}{\beta^4} C e^{-\frac{(E - E_o)^2}{2\sigma^2}} dE$$

where C is the normalizing constant.

For $\beta \simeq 1$, $\frac{1 - \beta^2}{\beta^4}$ may be replaced by $\left(\frac{m_o c^2}{E}\right)^2$.

Then:

$$A = \sum_i N_i Z_i^2 \left(\frac{e^2}{m_o c^2}\right)^2 \left(\frac{m_o c^2}{2}\right)^2 \int \frac{c}{E^2} e^{-\frac{(E - E_o)^2}{2\sigma^2}} dE \qquad (5)$$

This integral is computed in section C. 4. in terms of observable quantities.

3. Correction for Resolution

The resolution of an instrument is a measure of its accuracy in measurement. Analytical consideration is taken of the resolution by defining a resolution function $W(\delta, \delta')$ such that $W(\delta, \delta')\, d\delta'$ gives the probability that the variable δ will be observed between the limits δ' and $\delta' + d\delta'$. We now proceed to derive the correction necessary owing to the finite resolution involved in the measurement of the angles.

Let $W(\sin\delta, \sin\delta')$ = the resolution function,

$\sigma(\sin\delta)\, d(\sin\delta)$ = the theoretical differential cross section for scattering between $\sin\delta$ and $\sin\delta + d(\sin\delta)$,

$Q(\sin\delta')\, d(\sin\delta')$ = the observed differential cross section for scattering between $\sin\delta'$ and $\sin\delta' + d(\sin\delta')$,

σ_s = the standard deviation of the resolution function.

It follows that

$$Q(\sin\delta') = \int \sigma(\sin\delta)\, W(\sin\delta, \sin\delta')\, d(\sin\delta) \qquad (6)$$

We assume the error in measurement to be normally distributed, i.e.,

$$W(\sin\delta, \sin\delta') = C\, e^{-\frac{(\sin\delta - \sin\delta')^2}{2\sigma_s^2}}$$

where C is the normalizing factor. Since the effect of the resolution is important only at the smaller angles, a sufficient approximation for the cross section is given by

$$\sigma(\delta) = \frac{16\, A\, \pi}{\sin^3\delta} \qquad (7)$$

Equation (6) then becomes

$$Q(\sin\delta') = \int \frac{16\,A\,\pi}{\sin^3\delta}\, C\, e^{-\frac{(\sin\delta - \sin\delta')^2}{2\sigma_s^2}}\, d(\sin\delta) \quad .$$

Letting $\sin\delta - \sin\delta' = x$,

$$Q(\sin\delta') = 16A\pi C \int \frac{1}{(x + \sin\delta')^3}\, e^{-\frac{x^2}{2\sigma_s^2}}\, dx$$

$$= \frac{16A\pi C}{\sin^3\delta'} \int e^{-\frac{x^2}{\sigma_s^2}}\, dx \left(1 - \frac{3x}{\sin\delta'} + \frac{6x^2}{\sin^2\delta'} + \ldots\right)$$

$$= \frac{16A\pi}{\sin^3\delta'} \left(1 + 6\,\frac{\sigma_s^2}{\sin^2\delta'} + \ldots\right) \text{ to third order in } \sigma_s.$$

With the effects of resolution now considered and the theoretical expression now rendered in terms of the horizontally projected angle, the results of the nuclear scattering of 38.5-Mev electrons and 36.1-Mev positrons are tabulated in Fig. 6. From these results it may be concluded that within the statistics available and large-angle scattering of ~40-Mev electrons and positrons is fairly well described by the Rutherford scattering law. No further comparison was made with the charge-dependent Eq. (1), because in the region in which 95 percent of the statistics were gathered, Eq. (1) predicted only a 5 percent deviation.

4. Determination of the Particle Energies

The mean particle energy was determined from multiple-scattering measurements. On each of the three plates scanned forty tracks were chosen at random for measurement. The angle of scatter was determined by finding the second differences of track displacement, measured every 100 microns. For an electron

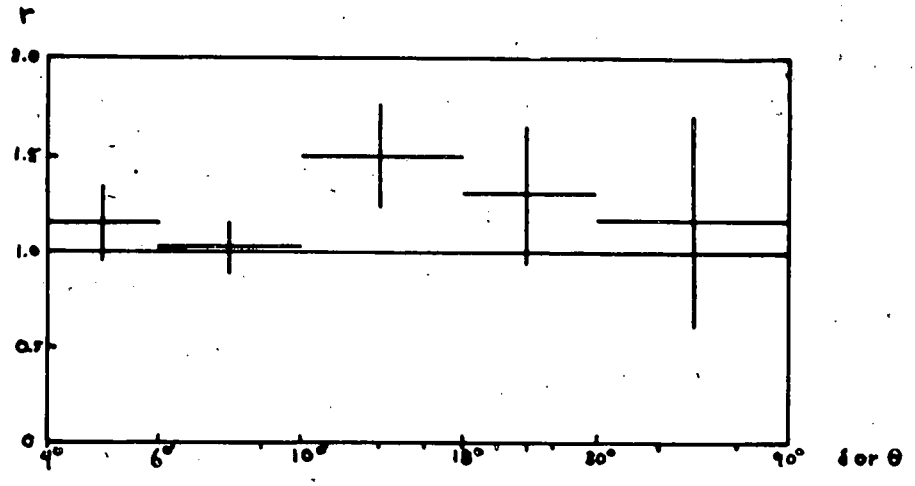

The ratio of observed positron-nuclear scattering to Rutherford scattering is plotted vs the angle (θ or δ) in degrees.

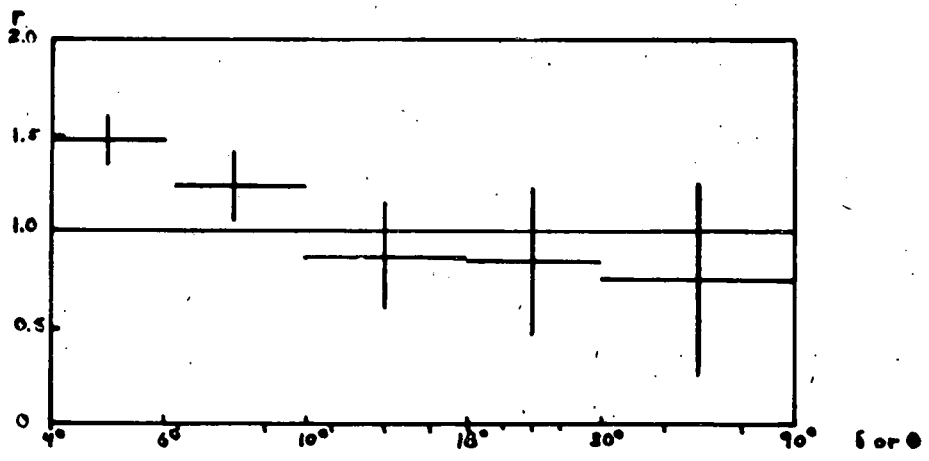

The ratio of observed electron-nuclear scattering to Rutherford scattering is plotted vs the angle (θ or δ) in degrees.

Fig. 6

of ~40 Mev, the expression relating the energy with the mean scattering angle is[6]

$$\langle |a| \rangle = \frac{K}{E} , \tag{8}$$

where E = particle energy,

K = the scattering factor,

$\langle |a| \rangle$ = mean angle of scatter, using a cell length of 100 microns.

The integral of Eq. (5) may now be computed as follows:

Let $p(a, E)\, da$ be the probability that a particle of energy E will be scattered between the angles of a and $a + da$ per unit cell length,

$q(a, a_o)\, da_o$ be the probability that an angle a will be observed between a_o and $a_o + da_o$.

Since $p(a, E)$ and $q(a, a_o)$ are normally distributed,

$$\langle a_o^2 \rangle_E = \langle a^2 \rangle_E + \langle a_r^2 \rangle \tag{9}$$

where $\langle a_r^2 \rangle$ is the mean square angle of error from the resolution function, $q(a, a_o)$.

$\langle a_o^2 \rangle_E$ is the second moment of the observed angles for a given E.

$\langle a^2 \rangle_E$ is the theoretical second moment of angles for a given E.

For a normal distribution,

$$\langle a^2 \rangle_E = \frac{\pi}{2} \langle |a| \rangle_E^2$$

and $$\langle a_r^2 \rangle = \frac{\pi}{2} \langle |a_r| \rangle^2 .$$

Therefore,

$$\left\langle a_o^2 \right\rangle_E - \frac{\pi}{2} \left\langle |a_r| \right\rangle^2 = \frac{\pi}{2} \left\langle |a| \right\rangle_E^2 ,$$

but

$$\left\langle |a| \right\rangle_E^2 = \frac{K^2}{E^2} ;$$

hence

$$\frac{\frac{2}{\pi} \left\langle a_o^2 \right\rangle_E - \left\langle |a_r| \right\rangle^2}{K^2} = \frac{1}{E^2}$$

Integrating over the normally distributed variable, E, we have

$$\int_{-\infty}^{\infty} \frac{C}{E^2} e^{\frac{-(E - E_o)^2}{2\sigma^2}} dE = \frac{\frac{2}{\pi} \left\langle a_o^2 \right\rangle - \left\langle |a_r| \right\rangle^2}{K^2} , \qquad (10)$$

where $\left\langle a_o^2 \right\rangle$ is the mean square of the observed angles over all tracks. This is the integral contained in the factor A.

(a) Determination of the mean angle of error

For measurements of cell lengths other than 100 microns, and on particles whose β is not 1, the relation between momentum and mean scattering angle is[7]

$$\left\langle |a| \right\rangle = \frac{K}{pv} \left(\frac{t}{100} \right)^{1/2} , \qquad (11)$$

where $\left\langle |a| \right\rangle$ = mean scattering angle in degrees

t = cell length in microns

K = scattering factor in $\frac{\text{Mev - degrees}}{\text{(micron)}}$

p = momentum of particle in $\frac{\text{Mev}}{c}$

v = velocity of particle in cm/sec

However, at these energies $v \simeq c$, i.e., E may be substituted for pv. Following Voyvodic[8], K, the scattering factor, varies as the 0.06 power of the cell length. For these measurements Voyvodic's value of 23.6 for K for 100-micron cells was used. The observed mean angle of scatter $\langle|a_o|\rangle$, is found by the relation $\langle|a_o|\rangle = \langle\frac{|D_o|}{t}\rangle$ where $\langle|D_o|\rangle$ is the mean second difference per cell length. The actual mean second difference, $\langle|D|\rangle$, is determined from the observed mean second difference by Eq. (9)

$$\langle|D_o|\rangle^2 = \langle|D|\rangle^2 + \langle|D_r|\rangle^2 \tag{12}$$

$\langle|D_r|\rangle$ is the mean error in the observations. It is due to the effects of observer resolution, microscope stage noise, finite grain size, and the distribution of grains about the actual path. By a procedure first described by Corson,[9] the error in the second differences, $\langle|D_r|\rangle$, is found as follows:

By squaring equation (8), $\langle|a|\rangle^2 = \frac{K^2}{E^2}\left(\frac{t}{100}\right)$, and substituting $\langle|a|\rangle^2 = \frac{\langle|D|\rangle^2}{t^2}$ and the proportionality of K to $t^{.06}$, we obtain

$$\langle|D|\rangle^2 = \frac{K'^2}{E^2}\, t^{3.12},$$

or, in terms of the error

$$\langle|D_o|\rangle^2 = At^{3.12} + \langle|D_r|\rangle^2 \tag{13}$$

It is seen that $\langle|D_o|\rangle$ is a linear function of $t^{3.12}$; the ordinate intercept of this function measures the "noise" squared. For the "noise" determination in this experiment the second differences were measured on the same track for 25-, 50-, 100-, 150-, and 200-micron cell lengths. By the method of least squares the ordinate intercept was then computed. The "noise", $\langle|D_r|\rangle$, amounted to 0.137 $\frac{\mu}{\text{cell}}$, or only ~2 percent of the observed second differences squared.

(b) Test for Emulsion Distortion

In order to make small-angle scattering measurements properly, it is essential that there be no emulsion distortion present. Emulsion distortion manifests itself by creating series of second differences whose signs are alike. To detect such an effect as this the second differences for each plate were plotted as in Fig. 7 with a new sign, the new sign being positive if the second difference had the same sign as the preceding one, and negative if it had a sign opposite that of the preceding one. If any emulsion distortion were present, the mean would be displaced from zero to some positive value. From the results it may be concluded that no appreciable emulsion distortion was present.

III. POSITRON ANNIHILATION IN FLIGHT

Six instances of positron annihilation in flight were observed in the positron plate during the course of the experiment. In each case an intensive investigation was undertaken in order to determine whether or not the positron reappeared at some point near by. Multiple-scattering measurements of the six tracks were carried out; the energies thus determined were consistent with the mean energy of other positrons in the plate. The annihilation events are compared in Table I with the two-quantum annihilation cross section given by Dirac.[10] The contribution to the cross section by zero- or one-quantum annihilation may be assumed negligible here.[11]

Observations by Colgate and Gilbert[12] of the annihilation cross section in Be and LiH were found to be consistent with the theory of Dirac. Three events at ~ 40 Mev and two at ~200 Mev, found by Barkas et al.[13] in nuclear emulsion, also were found to be consistent with theory.

Table I

Annihilation in Flight of Positrons

Mean Energy (Mev)	No. of Events	Track Length (cm.)	Obs. Ann. Length	Theor. Ann. Length
36.1 ± 5.3	6	185.5	30.9 ± 12.6	67.0

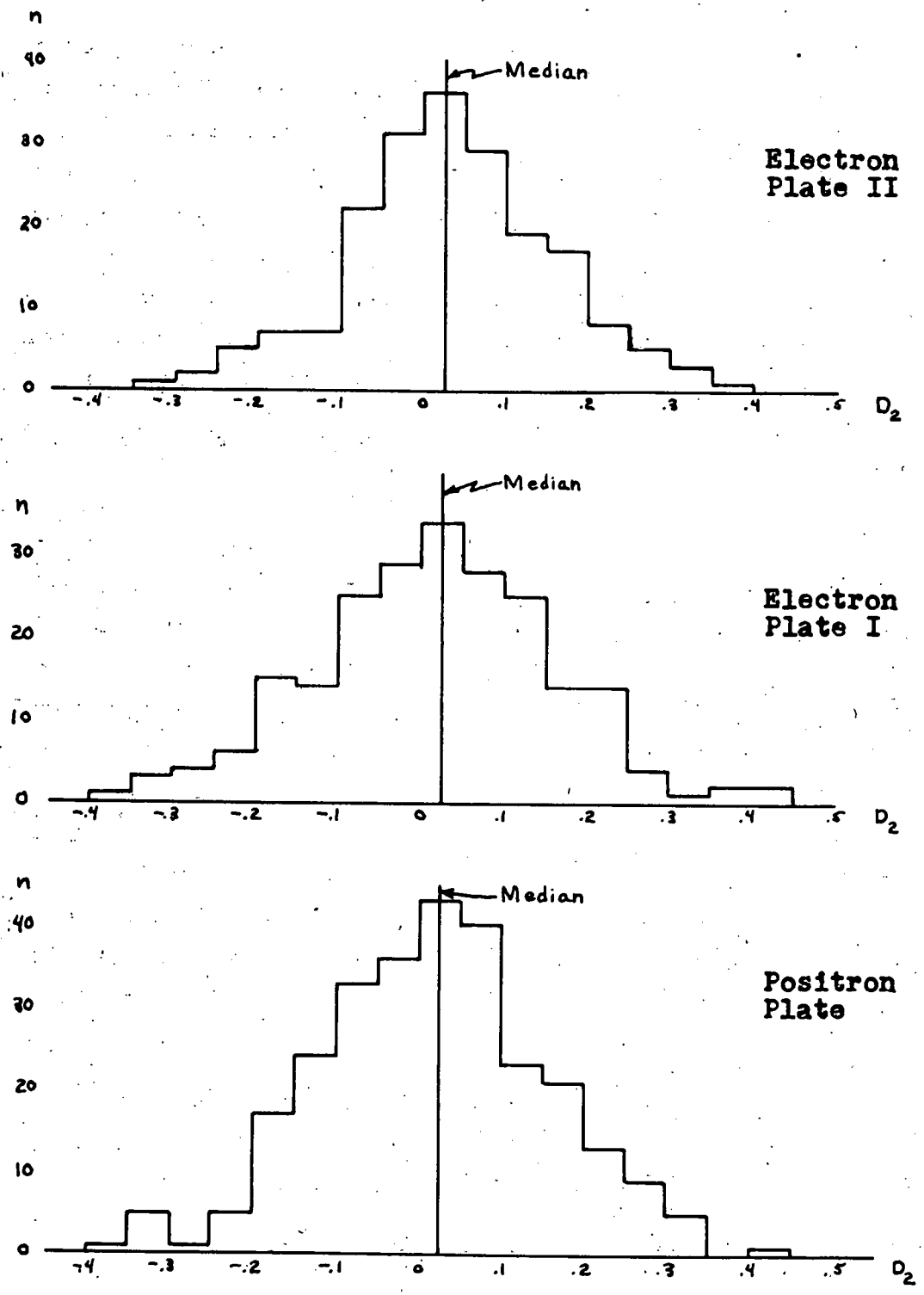

Fig. 7—Histograms of the number vs the second differences with sign as defined in the text for each of the three plates used.

IV. SMALL-ANGLE SCATTERING

The purpose of this portion of the paper is twofold: to create a scheme of analysis for gamma-ray spectra above a few Mev using the multiple-scattering information of the pair-production electrons, and, more specifically, to determine the energy distribution of gamma-rays coming from a Be target bombarded by 330-Mev protons.

A. Experimental Proceedure

A thin beryllium target 1mm x 1mm was bombarded by the 330-Mev proton beam of the 184-inch cyclotron. Gamma-rays emmitted at 90° from the incident beam were collimated by a long brass rectangular cylinder. The straight cylinder served to screen out all charged particles, which must travel in circular orbits in the magnetic field of the cyclotron. No charged particle, therefore, could travel from the slit to the detector. The gamma-rays were detected by the electron pairs they created in a G-5 nuclear emulsion plate 1 in. by 3 in. by 200 microns. The three-inch dimension was parallel to the gamma-ray paths, and the surface was inclined about 5° to them. (see Fig. 8). The plate had been previously "eradicated" and was developed according to the scheme outlined by Violet.[4]

The plate was scanned under 424-power magnification for pair-production events. The multiple scattering of each electron was then measured under 2250-power magnification. To determine the mean angle of scatter, 100-micron, 50-micron, and occasionally 25-micron cell lengths were used, depending upon the measurable track length available.

The total area observed was first scanned in strips perpendicular to the electron paths; 125 usable events were found in this way. It was then noticed that this method tended to select out the higher-energy members of the pair population, because these tend to be straighter and longer, and hence more easily found. Approximately one-third of the total area was then rescanned by the same observer. The technique was altered so that the new area was scanned in overlapping strips parallel to the direction of the gamma-ray paths; 28 new events and all the old events previously noted in this area were found. As was suspected, the mean energy of the newly discovered pairs was significantly lower than that found previously. The original distribution was then corrected by adding to it the weighted distribution of the new pairs found by the second technique.

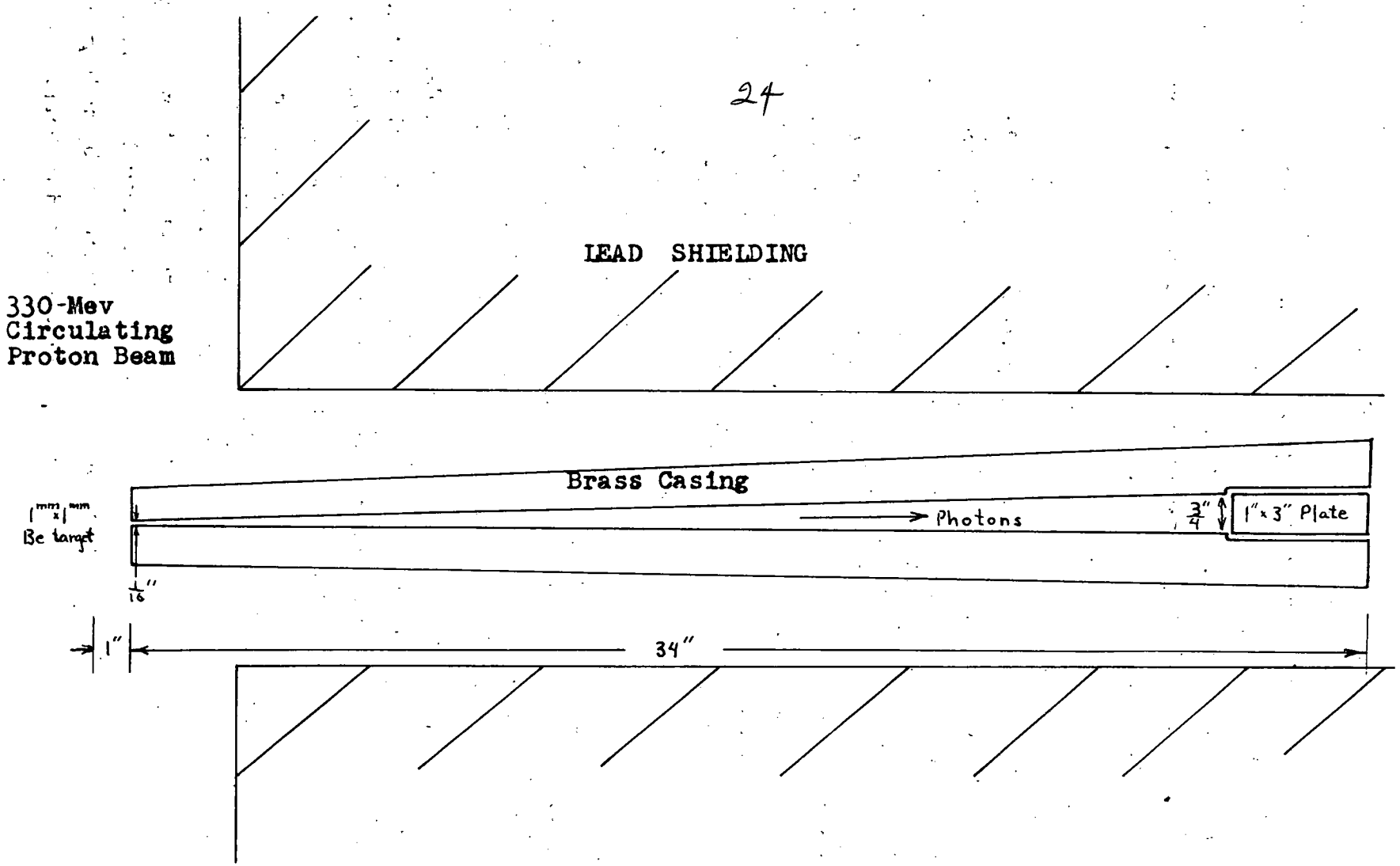

Fig. 8 — Experimental arrangement of gamma-ray detection equipment.

B. Data Analysis

In order that the observed data be interpreted properly, four important effects must be considered:

1. Ionization and Radiation Energy Loss

The first consideration is the energy loss due to ionization and to radiation. The ionization loss may be considered approximately constant for the energy regions involved. It is 4.90 Mev/cm as calculated by Violet.[14] The energy loss due to radiation may be computed from the expression

$$E = E_o e^{-\frac{x}{L}} \tag{14}$$

where E is the energy after traveling a distance x,

E_o is the incident energy,

L is the radiation length in emulsion.

Violet[14] has also calculated L to be 2.90 cm. The energies were corrected by adding to them the energy loss calculated for one-half the portion of the track measured. The energy distribution was then smoothed by weighting an element of the histogram by 6, the two adjacent elements by 4, and the next two elements by 1 (quartic smoothing). The energy distribution for the pairs corrected for radiation and ionization loss is shown in Fig. 9. The smoothed distribution is shown in Fig. 10.

2. Approximation of Scattering Formula

The second source of error arises because the scattering theory predicts the product of momentum and velocity rather than the energy (see Eq. 11), i.e.,

$$\langle |\alpha| \rangle \propto \frac{K}{p v} \tag{15}$$

where p = momentum,

v = velocity,

$\langle |\alpha| \rangle$ = mean angle of scattering,

K = scattering constant.

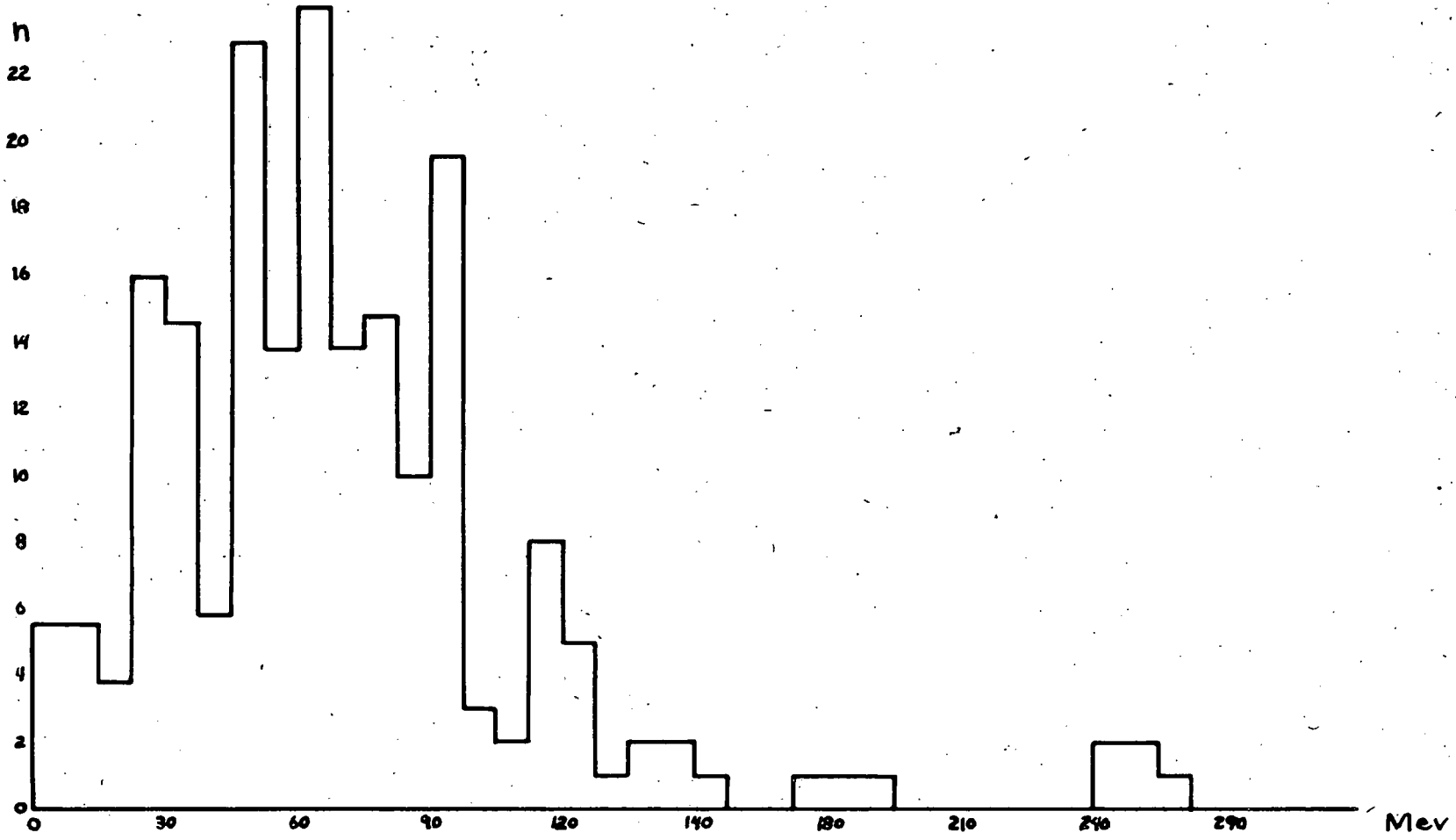

Fig. 9—Energy distribution of observed pairs corrected for ionization and radiation energy loss. The number vs energy in Mev are plotted.

Where particles have a velocity essentially that of light, it is entirely proper to replace pv by the energy. But when the velocity is appreciably below c, the approximation does not hold. Using the relativisitic expression for total energy as a function of momentum and rest energy,

$$(mc^2)^2 = (pc)^2 + (m_o c^2)^2,$$

we find that the total energy of an electron in terms of pv and the rest energy is

$$(mc^2) = \frac{pv \pm \sqrt{(pv)^2 + 4(m_o c^2)^2}}{2} \quad . \tag{16}$$

No correction was made to the data, however, for in no pair was the momentum of either electron sufficiently low to warrant correction.

3. Effects of Resolution

(a) Derivation of the resolution function

The energy of an electron is determined from the mean of the absolute value of the scattering angles measured at regular intervals (cell lengths). The distribution function of these angles is very nearly Gaussian. It is distributed about zero. Since a particular measurement of the scattering is an observation of a random variable, the mean of N such measurements is also an observation of some random variable, for which there must exist a distribution function. Specifically, the observed energies in a monoenergetic beam of electrons, obtained by making N measurements per track of the multiple scattering, will be distributed in some fashion about the actual energy. This distribution function is the "resolution" of the technique of measurement. It is derived as follows:

For a normally distributed (Gaussian) random variable of standard deviation σ, the distribution of the sample standard deviation squared, s^2, based upon N observations, is a chi-square distribution of (N-1) degrees of freedom.[15] Defined thus, the distribution is

$$f\left(N\frac{s^2}{\sigma^2}\right) = \frac{1}{2^{\frac{N-1}{2}}\,\Gamma\left(\frac{N-1}{2}\right)} \left(N\frac{s^2}{\sigma^2}\right)^{\frac{N-3}{2}} e^{-\frac{N}{2}\frac{s^2}{\sigma^2}} \tag{17}$$

For a normal distribution,

$$\sigma^2 = \frac{\pi}{2}\left\langle |a| \right\rangle^2$$

where $\left\langle |a| \right\rangle$ is the true mean of the angles of scatter.
Also from simple scattering theory we know that

$$E = \frac{K}{\left\langle |a| \right\rangle}$$

where E is the true particle energy,
K is the scattering factor.

The assumption is now made that s has the same relation to $\left\langle |a_o| \right\rangle$, i.e.,

$$s^2 \cong \frac{\pi}{2}\left\langle |a_o| \right\rangle^2,$$

where $\left\langle |a_o| \right\rangle$ is the observed mean of the scattering angles. We may also write

$$E' = \frac{K}{\left\langle |a_o| \right\rangle}$$

where E′ is the observed energy of the particle.
Finally we write

$$n\frac{s^2}{\sigma^2} \simeq n\frac{\left\langle |a_o| \right\rangle^2}{\left\langle |a| \right\rangle^2} = n\frac{E^2}{E'^2}$$

The distribution in terms of E and E′ becomes

$$f\left(n\frac{E^2}{E'^2}\right) = \frac{1}{2^{\frac{n-1}{2}}\,\Gamma\left(\frac{n-1}{2}\right)}\left(n\frac{E^2}{E'^2}\right)^{\frac{n-3}{2}} e^{-\frac{n}{2}\frac{E^2}{E'^2}} \qquad (18)$$

And the resolution function is derived by the following:

$$g(E, E')\,dE' = f\left(n\frac{E^2}{E'^2}\right)\; d\left(n\frac{E^2}{E'^2}\right)$$

$$= \frac{1}{2^{\frac{n-1}{2}}\;\Gamma\left(\frac{n-1}{2}\right)}\left(n\frac{E^2}{E'^2}\right)^{\frac{n-3}{2}}\; e^{-\frac{n}{2}\frac{E^2}{E'^2}}\left(n\frac{E^2\,dE'}{E'^3}\right)$$

$$= 2\,\frac{\left(\frac{n}{2}\right)^{\frac{n-1}{2}}}{\Gamma\left(\frac{n-1}{2}\right)}\left(\frac{E}{E'}\right)^{n}\; e^{-\frac{n}{2}\frac{E^2}{E'^2}}\;\frac{dE'}{E} \qquad (19)$$

This is the final form of the resolution function. In this form it is normalized so that

$$\int_0^\infty g(E, E')\,dE' = 1$$

Also: $g(E, E') = 0, \qquad -\infty < E < 0$ by definition.

If the distribution is considered as a function of $\frac{E'}{E}$, the half-width is a function solely of N. Hence the distribution function of the total energy of a pair of electrons may be well approximated by the proper choice of N. The expression for the probable uncertainty in energy of an electron is

$$\Delta E = \frac{.66}{\sqrt{N}}\;E \quad .$$

The probable uncertainty in energy of the electron pair is

$$\Delta E_p = \left[(\Delta E_1)^2 + (\Delta E_2)^2\right]^{1/2}$$

$$= \frac{.66}{\sqrt{N'}} E_p \qquad \text{where } N' \text{ is the effective number of measurements}$$

$$= \frac{.66}{\sqrt{N'}} (E_1 + E_2) = .66 \left[\frac{E_1^2}{N_1} + \frac{E_2^2}{N_2}\right]^{1/2},$$

hence

$$N' = \frac{(E_1 + E_2)^2}{E_1^2/N_1 + E_2^2/N_2}$$

Since N' varies from pair to pair, an effective $\langle N \rangle$ based upon the average probable error of the pairs must be used. Hence $\langle N \rangle$ is the value such that

$$\text{average probable error} = \frac{.66}{\sqrt{\langle N \rangle}} \,. \qquad (20)$$

$\langle N \rangle$ is found to be 13.5. The resolution function with $\langle N \rangle = 13.5$ is plotted in Fig. 11.

(b) Unfolding of the observed data.

A distribution function, $f(x)$, when detected with an instrument of resolution $g(x, x')$, is observed as a function $F(x')$ the relation being the following:

$$F(x') = \int_{-\infty}^{\infty} g(x, x')\, f(x)\, dx \qquad (21)$$

No general analytical procedure exists for solving this integral equation for $f(x)$. However, the following analytical approximation usually may be used: A family of functions $f_i(x)$, readily integrable with $g(x, x')$, are chosen.

It is our intent to synthesize f(x) from the $f_\iota(x)$, i.e.,

$$f(x) = \sum_\iota f_\iota(x) \tag{22}$$

The $f_\iota(x)$ do not necessarily have any physical significance. From the $f_\iota(x)$ a family of $F_\iota(x')$ are produced:

$$F_\iota(x') = \int_{-\infty}^{\infty} g(x, x')\, f_\iota(x)\, dx \tag{23}$$

The observed distribution function $F(x')$ is then synthesized from the family of $F_\iota(x')$ as follows:

$$F(x') = \sum_\iota F_\iota(x'); \tag{24}$$

f(x) may now be determined from (22). In my experiment it was found that the functions

$$f_\iota(E) = a_\iota \left(\frac{E}{\sigma_\iota}\right)^\iota e^{-\frac{E^2}{\sigma_\iota^2}} \tag{25}$$

were easily integrated with the resolution function. The family of $F_\iota(E')$ thus determined is

$$F_\iota(E') = a_\iota \frac{\Gamma\left(\frac{\langle N\rangle + \iota}{2}\right)}{\Gamma\left(\frac{\langle N\rangle - 1}{2}\right)} \left(\frac{\langle N\rangle}{2}\right)^{\frac{\langle N\rangle - 1}{2}} \frac{\left(\frac{E'}{\sigma_\iota}\right)^\iota}{\left(\frac{\langle N\rangle}{2} + \frac{E'^2}{\sigma_\iota^2}\right)^{\frac{\langle N\rangle + \iota}{2}}} \tag{26}$$

Four terms were used for the synthesis. The observed distribution and the synthesized analytical function are plotted together in Fig. 10. The resulting expression for f(E), the true energy distribution, becomes:

$$f(E) = 7.69\left(\frac{E}{22.5}\right) e^{-\left(\frac{E}{22.5}\right)^2} + 12.20\left(\frac{E}{30}\right)^4 e^{-\left(\frac{E}{30}\right)^2}$$

$$+ 1.79\left(\frac{E}{38.0}\right)^8 e^{-\left(\frac{E}{38.0}\right)^2} + .00384\left(\frac{E}{42.9}\right)^{12} e^{-\left(\frac{E}{42.9}\right)^2} \qquad (27)$$

(E in Mev)

and is plotted in Fig. 12.

4. Correction for Absorption in Emulsion

The fourth correction necessary is due to the fact that the mean free path for pair production in nuclear emulsion is not independent of photon energy. Heitler[16] has computed this dependence for some elements by a numerical integration of the quantum-mechanical expression for pair production. In order to compute the dependence for photons penetrating the muxture of elements that constitutes a nuclear emulsion, it was necessary to interpolate between his curves and create curves for all the elements involved in a nuclear emulsion. The total absorption in emulsion is merely the sum of the absorptions of all the elements involved. The resulting reciprocal free path for pair production in nuclear emulsion as a function of energy is shown in Fig. 13. The corrected energy distribution of gamma-rays coming from a beryllium target is shown in Fig. 14.

These results are interpreted as the energy distribution of decay photons coming from π^o mesons created in the target. It is expected that the peak from the π^o meson photons is of the order of 70 Mev. The observed peak lies in the range of 45 to 75 Mev. The curve is not as wide, however, as that found by Crandall[17] when he studied the decay photons of π^o mesons coming at 90^o from carbon at these energies. The very low-energy photons may be attributed to nuclear gamma-rays as well as bremsstrahlung.

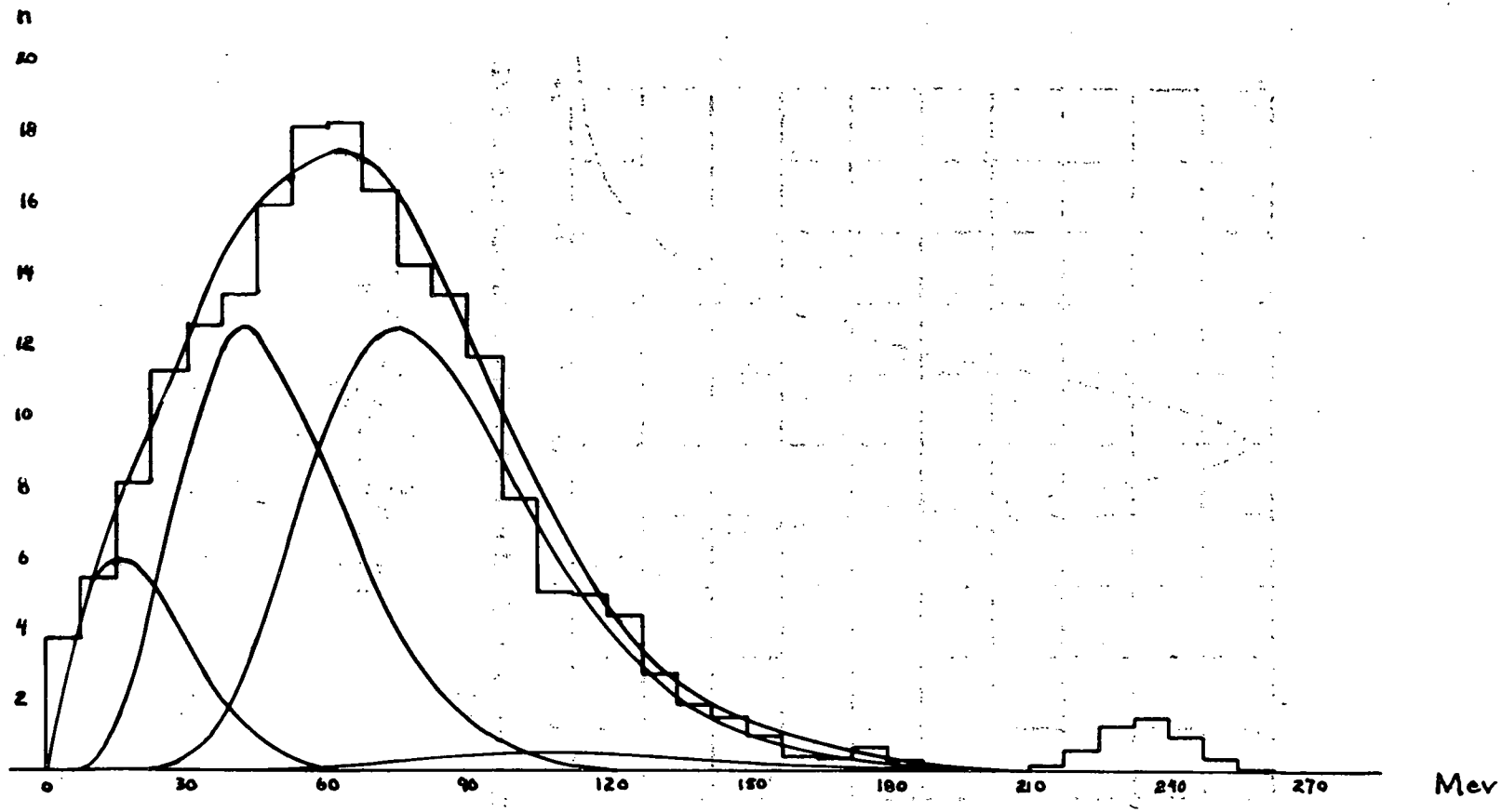

Fig. 10—Smoothed histogram of number of pairs vs energy in Mev. Superimposed is analytical approximation and components of analysis as described in text.

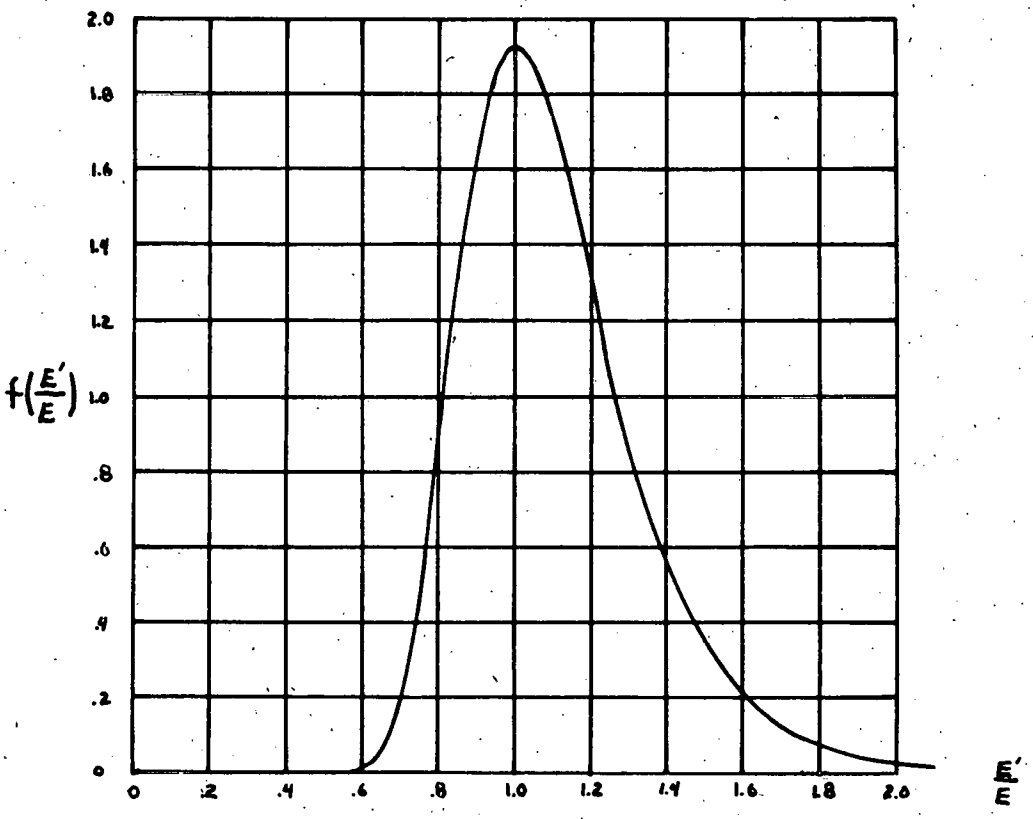

Fig. 11—Normalized resolution curve as function of E′/E for n = 13.5.

$$f\left(\frac{E'}{E}\right) = \frac{2\left(\frac{n}{2}\right)^{\frac{n-1}{2}}}{\Gamma\left(\frac{n-1}{2}\right)}\left(\frac{E}{E'}\right)^{n} e^{-\frac{n}{2}\frac{E^2}{E'^2}}$$

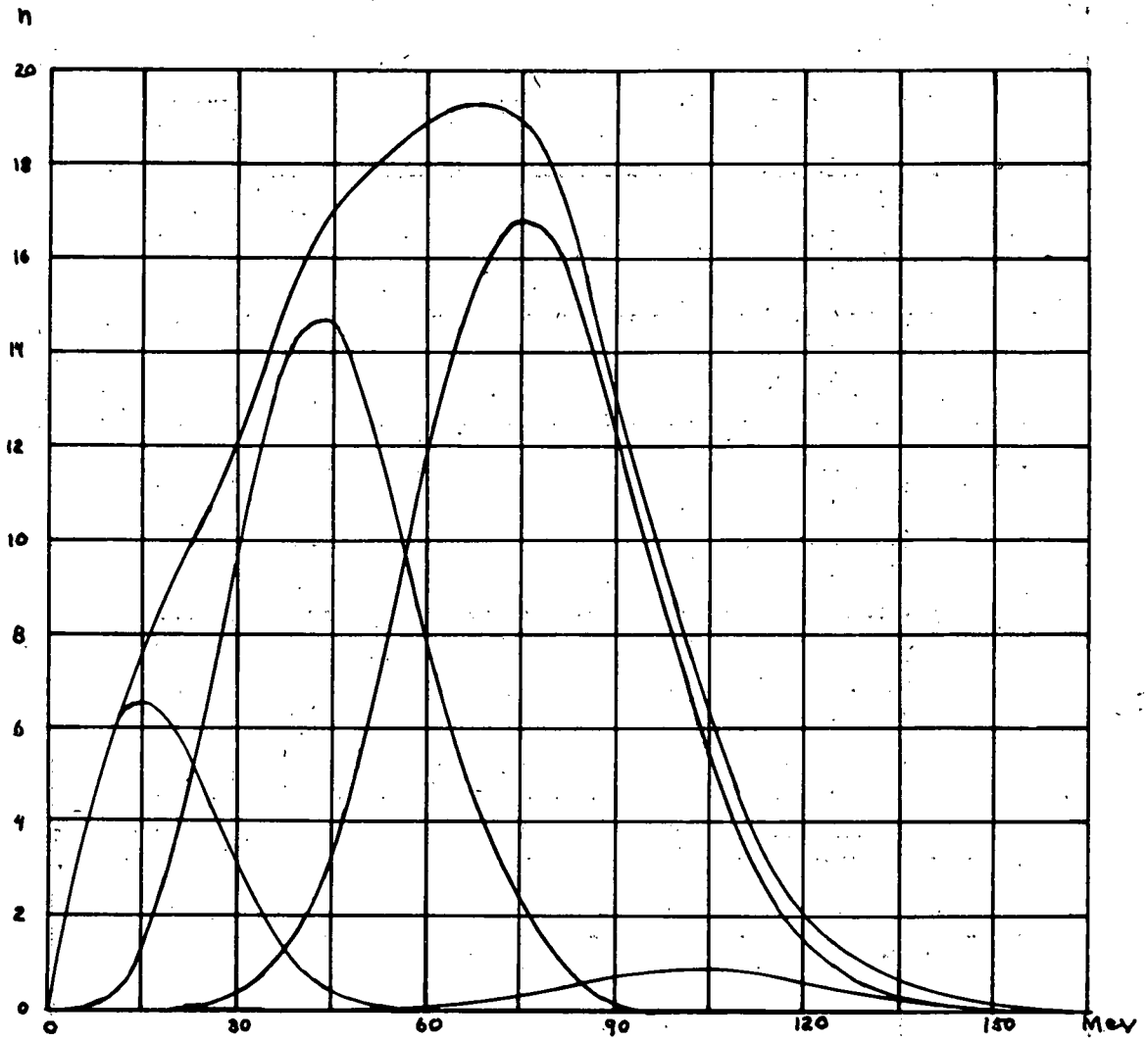

Fig. 12—Energy distribution of pairs corrected for resolution, and components out of which curve is synthesized.

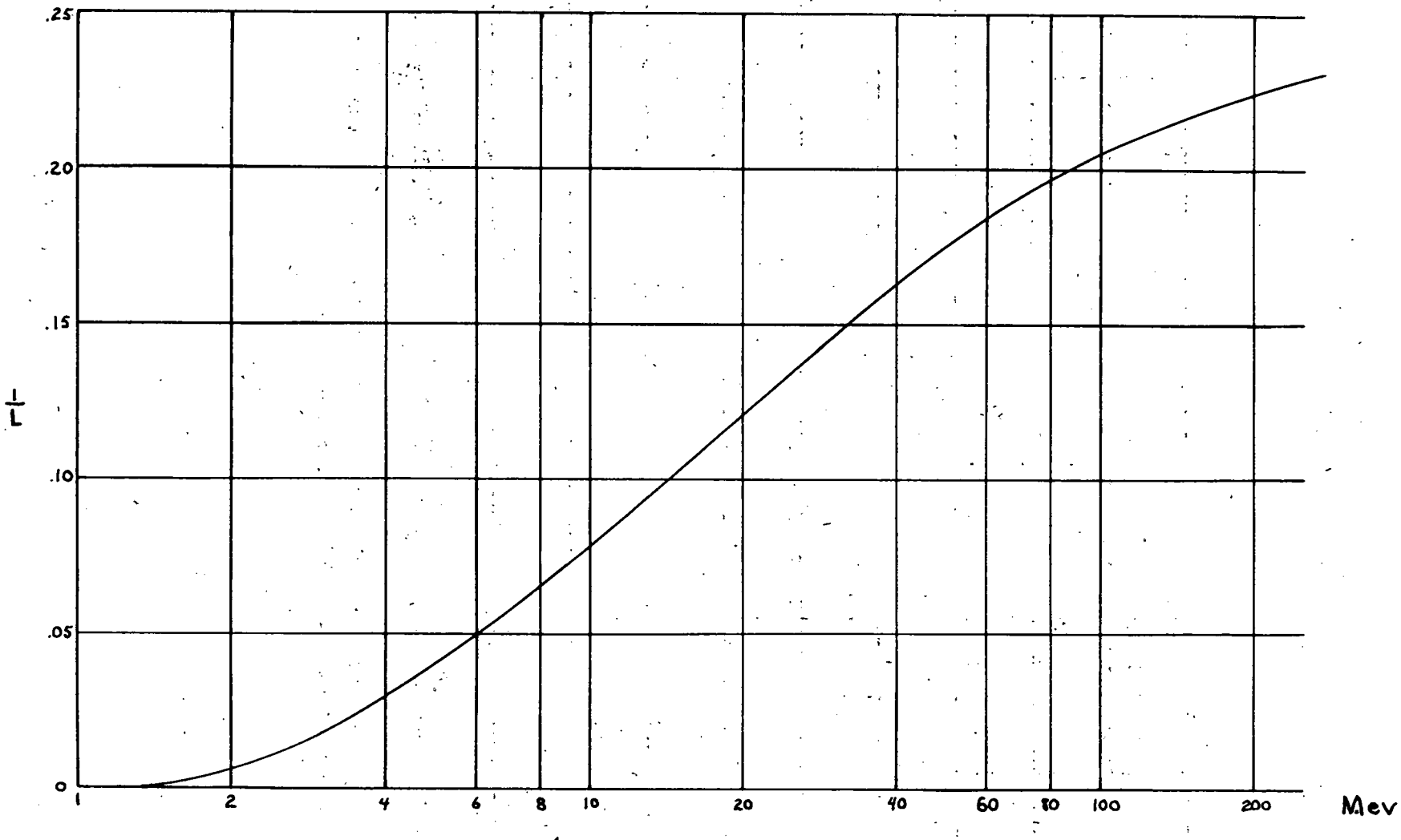

Fig. 13—Reciprocal free path (cm^{-1}) in nuclear emulsion for pair production vs photon energy in Mev.

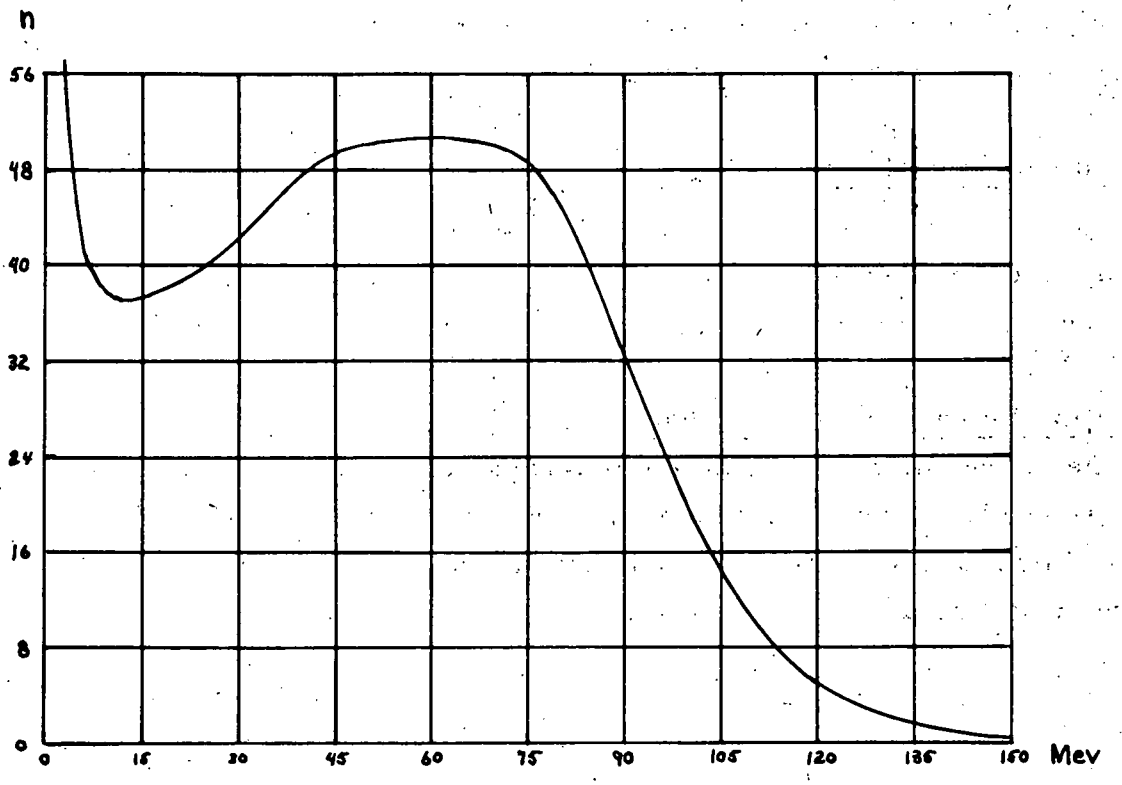

Fig. 14 — Energy distribution in Mev of photons at 90 degrees from a beryllium target.

V. SUMMARY

A. Large-Angle Scattering

The large-angle nuclear scattering of ~40-Mev electrons and of ~40-Mev positrons penetrating nuclear emulsion has been measured and shown to be fairly well described by the Rutherford scattering law. The Rutherford formula for scattering has been expressed in terms of a horizontally projected angle, and consideration has been taken of the effects of the observer resolution and of the spread in energy of the particles available.

B. Positron Annihilation in Flight

The observed annihilation length has been compared with the two-quantum annihilation cross section of Dirac, and is found to agree within an order of magnitude.

C. Multiple Scattering of Electrons

The energy distribution of gamma-rays coming from a Be target has been determined. The resolution function for the energy distribution of electrons as measured by multiple scattering has been derived, and a method of "unfolding" observed data has been demonstrated.

VI. ACKNOWLEDGMENTS

I am indebted to Dr. Walter H. Barkas for suggesting these problems to me, and for his continued advice, leadership, and inspiration, which helped bring this work to its conclusion.

I sincerely wish to thank Dr. Charles E. Violet and Mr. F. C. Gilbert for the plates used for the first section, and to Dr. Harry H. Heckman for the plate used in the second portion. To these people as well as to Mr. L. Evan Bailey gratitude is expressed for many enlightening discussions and for assistance in editing the work.

I also wish to thank Mr. Roland P. Michaelis for the photomicrography work.

To Mrs. Jennie Louie go many thanks for her meticulous scanning, indeed a major contribution to this paper.

And finally to my very patient wife, Ruth-Anne, for the many long hours of typing and editing of this paper, go my heartfelt thanks.

VII. REFERENCES

1. N. F. Mott, Proc. Roy. Soc. A124, 426 (1929).
2. Mott and Massey, Theory of Atomic Collisions, Oxford, (1949)
3. H. J. Lipkins, Doctoral Thesis, Princeton University, pp 1-3, (1950)
4. C. E. Violet, Interactions of Fast Electrons and Positrons with Matter, Thesis, Radiation Laboratory, University of California, Report No. UCRL-2163, April 3, 1953, p. 7.
5. W. H. Barkas, UCRL Film Program Notebook 30, 182 (1948)
6. Y. Goldschmidt-Clermont, Nuovo Cimento VII, 331 (1950)
7. L. Voyvodic and E. Pickup, Phys. Rev. 85, 91 (1952)
8. ibid, p. 94
9. D. R. Corson, Phys. Rev. 80, 303 (1950)
10. P. A. M. Dirac, Proc. Camb. Phil. Soc. 26, 361 (1930).
11. W. Heitler, The Quantum Theory of Radiation, Oxford, 1944, p. 209
12. S. A. Colgate and F. C. Gilbert, Phys. Rev. 89, 790 (1952)
13. Barkas, Deutsch, Gilbert, and Violet, Phys. Rev. 88, 1435 (1952)
14. C. E. Violet, Interaction of Fast Electrons and Positrons with Matter, Thesis, Radiation Laboratory, University of California, Report No. UCRL 2163, April 3, 1953, p. 35.
15. P. G. Hoel, Introduction to Mathematical Statistics, Wiley and Sons, London, 1947, p. 138.
16. W. Heitler, The Quantum Theory of Radiation, Oxford, 1944, p. 201.
17. W. E. Crandall and B. J. Moyer, Characteristics of Neutral Meson Production in the Proton Bombardment of Carbon Nuclei, Radiation Laboratory, University of California, Report No. UCRL 2110, Feb. 13, 1953

Information Division
11-17-53 JGT

THIS PAGE
WAS INTENTIONALLY
LEFT BLANK